British Journal of Pharmacology

DOI:10.1111/j.1476-5381.2012.02059.x
www.brjpharmacol.org

Themed Section: Cannabinoids 2012

RESEARCH PAPER

The antinociceptive triterpene β-amyrin inhibits 2-arachidonoylglycerol (2-AG) hydrolysis without directly targeting cannabinoid receptors

A Chicca, J Marazzi and J Gertsch

Institute of Biochemistry and Molecular Medicine, National Centre of Competence in Research NCCR TransCure, University of Bern, Bern, Switzerland

Correspondence
Jürg Gertsch, Institute of Biochemistry and Molecular Medicine, National Centre of Competence in Research NCCR TransCure, Bühlstrasse 28, University of Bern, 3012 Bern, Switzerland. E-mail: gertsch@ibmm.unibe.ch

Keywords
amyrin; 2-AG; CB_1 receptor; endocannabinoid system; hydrolases; monoacyl glycerol lipase; pristimerin; triterpene

Received
10 December 2011
Revised
15 May 2012
Accepted
16 May 2012

BACKGROUND AND PURPOSE

Pharmacological activation of cannabinoid CB_1 and CB_2 receptors is a therapeutic strategy to treat chronic and inflammatory pain. It was recently reported that a mixture of natural triterpenes α- and β-amyrin bound selectively to CB_1 receptors with a subnanomolar K_i value (133 pM). Orally administered α/β-amyrin inhibited inflammatory and persistent neuropathic pain in mice through both CB_1 and CB_2 receptors. Here, we investigated effects of amyrins on the major components of the endocannabinoid system.

EXPERIMENTAL APPROACH

We measured CB receptor binding interactions of α- and β-amyrin in validated binding assays using *h*CB_1 and *h*CB_2 transfected CHO-K1 cells. Effects on endocannabinoid transport in U937 cells and breakdown using homogenates of BV2 cells and pig brain, as well as purified enzymes, were also studied.

KEY RESULTS

There was no binding of either α- or β-amyrin to *h*CB receptors in our assays (K_i > 10 μM). The triterpene β-amyrin potently inhibited 2-arachidonoyl glycerol (2-AG) hydrolysis in pig brain homogenates, but not that of anandamide. Although β-amyrin only weakly inhibited purified human monoacylglycerol lipase (MAGL), it also inhibited α,β-hydrolases and more potently inhibited 2-AG breakdown than α-amyrin and the MAGL inhibitor pristimerin in BV2 cell and pig brain homogenates.

CONCLUSIONS AND IMPLICATIONS

We propose that β-amyrin exerts its analgesic and anti-inflammatory pharmacological effects via indirect cannabimimetic mechanisms by inhibiting the degradation of the endocannabinoid 2-AG without interacting directly with CB receptors. Triterpenoids appear to offer a very broad and largely unexplored scaffold for inhibitors of the enzymic degradation of 2-AG.

LINKED ARTICLES

This article is part of a themed section on Cannabinoids. To view the other articles in this section visit http://dx.doi.org/10.1111/bph.2012.167.issue-8

Abbreviations

Δ^9-THC, Δ^9-tetrahydrocannabinol; CP55940, -(–)-cis-3-[2-hydroxy-4-(1,1-dimethylheptyl)phenyl]-trans-4-(3-hydroxypropyl)cyclohexanol; ECS, endocannabinoid system; FAAH, fatty acid amide hydrolase; JZL184, 4-nitrophenyl-4-[bis(1,3-benzodioxol-5-yl)(hydroxy)methyl]piperidine-1-carboxylate; MAFP, methyl arachidonylfluorophosphonate; MAGL, monoacylglycerol lipase; SR141716A, *N*-(piperidin-1-yl)-5-(4-chlorophenyl)-1-(2,4-dichlorophenyl)-4-methyl-1H-pyrazole-3-carboxamide hydrochloride; THL, tetrahydrolipstatin; T_{max}, time to maximal concentration in plasma (pharmacokinetic parameter); WIN55,212-2, (R)-(+)-[2,3-dihydro-5-methyl-3-(4-morpholinylmethyl)pyrrolo-[1,2,3-de]-1,4-benzoxazin-6-yl]-1-naphtaleneylmethanone

Introduction

Cannabinoid CB_1 receptors exert a range of central and peripheral pharmacological effects including analgesia (Pacher *et al.*, 2006; Guindon and Hohmann, 2008; Bisogno and Di Marzo, 2010; receptor nomenclature follows Alexander *et al.*, 2011). Activation of CB_1 receptors in the CNS typically leads to pronounced psychomodulatory effects, including inhibition of locomotion, catalepsy, reduction of body temperature and antinociception (the tetrad effect) (Fride *et al.*, 2006; Pertwee, 2009; Pertwee *et al.*, 2010). While there is a wide range of synthetic CB_1 receptor agonists, Δ^9-tetrahydrocannabinol (Δ^9-THC) from the plant *Cannabis sativa* L and closely related secondary metabolites are the only natural products known so far to potently activate the CB_1 receptor (Gertsch *et al.*, 2010). We were therefore intrigued by a recent study by Da Silva *et al.* (2011) reporting the ultrapotent and highly selective interaction (activation) of a 1:1 mixture of the triterpenes α/β-amyrin with the CB_1 receptor without causing behavioural effects. The pentacyclic triterpene β-amyrin is a primary cyclization product derived from squalene (Rees *et al.*, 1968) and thus a canonical and widely occurring triterpenoid precursor for a number of pentacyclic terpenes. Anti-inflammatory and antinociceptive properties of β-amyrin have been reported previously (Akihisa *et al.*, 1996; Holanda Pinto *et al.*, 2008; Melo *et al.*, 2010; 2011), but a feasible mechanism of action is lacking. In the study by da Silva *et al.*, oral α/β-amyrin chronically administered at 30 $mg \cdot kg^{-1}$ inhibited mechanical and thermal hyperalgesia and inflammation induced by complete Freund's adjuvant and by partial sciatic nerve ligation. Remarkably, in this study, the α/β-amyrin mixture exhibited a very potent binding to CB_1 receptors with a K_i value of 133 pM, which is approximately 200–300-fold more potent than Δ^9-THC. Moreover, in contrast to Δ^9-THC and the endogenous ligand 2-arachidonoyol glycerol (2-AG), α/β-amyrin showed an unusual 15 000-fold binding selectivity to CB_1 receptors over CB_2 receptors (Da Silva *et al.*, 2011). Notably, there are relatively few subnanomolar CB_1 receptor ligands known, such as, for example CE-178253 and CP-945,598, which were synthesized at Pfizer (Griffith *et al.*, 2009; Hadcock *et al.*, 2010), JWH182 from Huffman Laboratories (Huffman *et al.*, 2005), or AM4030a and others from the Makriyannis laboratory (Papahatjis *et al.*, 1998; Thakur *et al.*, 2002). Thus, the finding that a canonical plant triterpene exhibits such potent and selective binding interactions with CB_1 over CB_2 receptors is of great interest. The authors concluded that the CB_1 receptor interaction (as detected in their binding assays) was the major mechanism of action. Although not shown in their study, they assumed that α/β-amyrin activates CB_1 receptors. In their report, pretreatment with both CB_1 or CB_2 antagonists and gene knockdowns of both receptors significantly inhibited the antinociceptive effect of α/β-amyrin, indicating direct or indirect effects on CB receptors.

The study by da Silva *et al.* (2011) raises several basic questions that need to be addressed before classifying the amyrins as novel CB_1 receptor-selective agonists. In order to understand the actual mechanism of action, α-amyrin (vicinal methyls in A ring) and β-amyrin (geminal methyls in A ring) should be studied separately as both compounds are commercially available in purities >95% from Sigma-Aldrich and other providers. The CB_1 and CB_2 receptor binding interactions were performed in rat brain and mouse spleen homogenates, respectively, using the specific radioligands [^{3}H]-SR141716A (rimonabant) and [^{3}H]-CP55,940. Because both tissues potentially show a high degree of non-specific binding and the radioligands may have additional targets (Breivogel, 2006), it is important to reproduce the ultrapotent CB_1 receptor binding interaction in more defined recombinant systems, using additional controls. Because CB_1 receptor agonists typically trigger a $G_{i/o}$ protein-mediated signalling, it would be interesting to know whether α/β-amyrins are full or partial agonists. In light of the CB receptor non-specific pharmacology (the antinociceptive effects were inhibited by both CB_1 and CB_2 receptor antagonists), which is in conflict with a purely CB_1 receptor-mediated mechanism, also, other targets related to endocannabinoid breakdown should be considered. In the present study, we have addressed these issues and now provide an alternative cannabimimetic mechanism of action of α/β-amyrin, which is able to explain, at least in part, the pharmacology of the amyrins. Our results show a potent inhibition of 2-AG hydrolysis by β-amyrin in brain tissue and point out a significant difference in the inhibitory potency between the two structural isomers.

Methods

Cell culture

Human leukemia monocytic lymphoma U937 cells were purchased from American Type Culture Collection (Manassas, VA, USA) and were grown in RPMI 1640 medium supplemented with 10% fetal bovine serum, 1 $g \cdot mL^{-1}$ fungizone (amphotericin B), 100 $units \cdot mL^{-1}$ penicillin, 100 $g \cdot mL^{-1}$ streptomycin and 2 mM L-glutamine (all from Invitrogen, Carlsbad, CA, USA). The *h*CB_1- or *h*CB_2-expressing CHO-K1 cells (Raduner *et al.*, 2006) were grown in the same medium as the U937 cells, but supplemented with 400 $\mu g \cdot mL^{-1}$ G418 (10131-027; Invitrogen). Cells were grown in a humidified incubator at 37°C and 5% CO2.

Membrane preparation

CHO-K1 cells stably transfected with *h*CB_1 or *h*CB_2 receptors were seeded in a T150 cm^2 flask until reaching confluence and then collected by scraping. The cell suspension was resuspended in 1.5 mL of homogenization solution (50 mM Tris-HCl, 1 mM EDTA, 3 mM $MgCl_2$, pH 7.5) and homogenized on ice using a Dounce homogenizer with 50 gentle strokes. The cell homogenate was then centrifuged at 800 × *g* for 8 min at 4°C. The supernatant was collected (membrane fraction 1) and the pellet resuspended in 700 µL of homogenization solution, passed through a syringe 10 times, and centrifuged at 800 × *g* for 8 min at 4°C. The supernatant was collected (membrane fraction 2) while the pellet underwent the same operations described earlier. The supernatant was collected (membrane fraction 3) and pooled with membrane fraction 2 (membrane fraction 4). Membrane fractions 1 and 4 were then centrifuged at 3500 × *g* for 10 min at 4°C, the supernatant was discarded and both pellets resuspended in homogenization solution to a final volume of 600 µL ('crude

membrane fraction'). Protein concentration was determined using the Bradford method and aliquots stored at –80°C.

Radioligand binding assays on hCB_1 and hCB_2 receptors

Receptor-binding experiments were performed with membrane preparations as previously reported (Raduner *et al.*, 2006; Gertsch *et al.*, 2008). Briefly, 18 μg of crude membrane expressing *h*CB_1 or *h*CB_2 receptors (prepared as described earlier) were resuspended in 500 μL of binding buffer (50 mM Tris-HCl, 2.5 mM EDTA, 5 mM $MgCl_2$, 0.5 mg·mL^{-1} fatty acid-free BSA, pH 7.4) in silanized glass tubes and co-incubated with different concentrations of α-amyrin, β-amyrin or WIN55,512-2 and 0.5 nM of [^{3}H]-CP-55 940 (168 Ci·mmol^{-1}) for 2 h at 30°C with shaking. Non-specific binding of the radioligand was determined in the presence of 10 μM of WIN55,512-2. Non-specific binding was around 5%. After the incubation time, membrane suspensions were rapidly filtered through a 0.05% polyethyleneimine presoaked 96-well microplate bonded with GF/B glass fibre filters (UniFilter-96 GF/B, PerkinElmer Life Sciences) under vacuum and washed 12 times with 167 μL of ice-cold washing buffer (50 mM Tris-HCl, 2.5 mM EGTA, 5 mM $MgCl_2$, 0.5% fatty acid free BSA, pH 7.4). Filters were added to 40 μL of MicroScint20 scintillation liquid and radioactivity measured with the 1450 MicroBeta Trilux top counter (PerkinElmer Life Sciences). Data were collected from three independent experiments performed in triplicate and the non-specific binding was subtracted. Results were expressed as [^{3}H]-CP-55 940 bound as % of binding in vehicle-treated samples.

Fatty acid amide hydrolase (FAAH) activity assay

The experiments were performed as previously described (Chicca *et al.*, 2009). Briefly, FAAH activity, which is responsible for most of the anandamide (AEA) breakdown, was assessed using a cellular homogenate from fresh pig brains obtained from the slaughterhouse. Different concentrations of α-amyrin, β-amyrin or 1 μM PMSF (as the positive control) in 2.5 μL DMSO were preincubated at 37°C for 20 min with 195 μL of diluted pig brain homogenate in 10 mM Tris–HCl and 1 mM EDTA, pH 7.6 (corresponding to 200 μg of total protein) and 1% w/v fatty acid-free BSA (Sigma, St. Louis, MO, USA). Successively, 2.5 μL of non-radioactive AEA and [ethanolamine-1-^{3}H]-AEA (40–60 Ci·mmol^{-1}) mixture was added to the homogenate (final concentration in the assay was 2 μM) and incubated for 10 min at 37°C with shaking. After the incubation time, 400 μL of a methanol : chloroform mixture 1:1 (v/v) was added at each sample, vigorously vortexed and centrifuged at 10 000 × *g* for 10 min at 4°C to separate aqueous and organic phases. The radioactivity associated with the hydrolysis product [^{3}H]-ethanolamine was measured after addition of 3 mL of Ultima Gold scintillation liquid (PerkinElmer Life Sciences) to the aqueous phase, using a Tri-Carb 2100 TR scintillation counter (PerkinElmer Life Sciences). Data were collected from three independent experiments performed in triplicate and results were expressed as FAAH activity, relative to that in vehicle-treated samples (= 100%).

Assay of [^{3}H]-2-oleoyl glycerol (2-OG) hydrolysis in pig brain homogenate

The experiments were performed as recently described (Björklund *et al.*, 2010) with some minor changes. In brief, 195 μL (corresponding to 200 μg of total protein) of diluted pig brain homogenate in 10 mM Tris–HCl, 1 mM EDTA, plus 0.1% w/v fatty acid-free BSA pH 7.4 was preincubated for 30 min at 37°C with different concentrations (2.5 μL) of α-amyrin, β-amyrin, JZL184 or the mixture of α,β-hydrolases (ABHD) -6 and –12 inhibitors (10 μM WWL70 and 20 μM THL, respectively) plus 1 μM JZL184 as the positive control for the maximal inhibition of 2-AG hydrolysis. After the preincubation, 2.5 μL of nonradioactive (2-OG) and [1,2,3-^{3}H]-2-OG (60 Ci·mmol^{-1}) mixture was added to the homogenate (final concentration in the assay was 10 μM) and incubated for 10 min at 37°C with shaking. Successively, 400 μL of a methanol : chloroform mixture 1:1 (v/v) was added and, after vigorous vortexing, aqueous and organic phases were separated by centrifugation at 10 000 × *g* for 10 min at 4°C. The radioactivity associated with [^{3}H]-glycerol formation was measured after addition of 3 mL of Ultima Gold scintillation liquid (PerkinElmer Life Sciences) to the aqueous phase, using a Tri-Carb 2100 TR scintillation counter (PerkinElmer Life Sciences). Data were collected from three independent experiments performed in triplicate and results were expressed as [^{3}H]-glycerol formation, relative to that in vehicle-treated samples (=100%).

[^{3}H]-2-OG hydrolysis in homogenates of BV2 cells

The method was adapted from Marrs *et al.* (2010). In brief, BV2 cell homogenates (100 μg of total protein) were added to silanized plastic tubes containing 100 μL of buffer (10 mM Tris-HCl, 1 mM EDTA (pH 7.4) supplemented with 0.1% fatty acid-free BSA. The homogenate was preincubated for 30 min at 37°C with shaking in presence of 1 μM URB597 (to block FAAH activity) and different concentrations of amyrins, JZL184, WWL70, pristimerin or vehicle. Subsequently 2.5 nM of [^{3}H]-2-OG was added and the tubes incubated for 15 min at 37°C with shaking. The reaction was stopped by adding 300 μL of a methanol : chloroform mixture 1:1 (v/v) and vortexing. To separate organic and aqueous phases, the tubes were centrifuged for 10 min at 10 000 × *g* at 4°C. The upper aqueous phase was transferred to scintillation tubes and-mixed with 3 mL of Ultima Gold scintillation liquid (PerkinElmer Life Sciences). Radioactivity was measured using a Beckman LS6500 scintillation counter. Data were collected from three independent experiments each performed in triplicate and results were expressed as [^{3}H]-glycerol formation, relative to that in vehicle-treated samples (=100%).

Monoacylglycerol lipase (MAGL) activity assay

Purified recombinant human MAGL (*h*MAGL) was purchased from Cayman Chemicals. MAGL esterase activity was assessed as previously reported (King *et al.*, 2007; 2009a; Björklund *et al.*, 2010). The reaction consisted of 196 μL assay buffer (10 mM Tris-HCl 1 mM EDTA pH 7.4, plus 0.1% fatty acid-free BSA) containing 25 ng of purified *h*MAGL and 2 μL of JZL184, α-amyrin, β-amyrin, pristimerin or vehicle and

2.5 nM [^{3}H]-2-OG (2 μL). To assess the time-dependency of MAGL inhibition, the reaction was incubated for periods between 1 and 60 min. To assess the reversibility of MAGL inhibition, we performed an assay reported previously (King *et al.*, 2009b). The reaction mixture was incubated for 15 min at 37°C and then stopped by adding 400 μL of chloroform : methanol mixture 1:1 (v/v). Tubes were vortexed and centrifuged for 10 min at 10 000 × *g* at 4°C. Finally, the upper aqueous phase was transferred in scintillation tubes and mixed with 3 mL of Ultima Gold scintillation liquid (PerkinElmer Life Sciences). Radioactivity was measured using a Beckman LS6500 scintillation counter. Data were collected from two independent experiments performed in triplicates and the results were expressed as % [^{3}H]-glycerol formation, relative to that in vehicle-treated samples (=100%).

[^{3}H]-2-AG uptake into U937 cells

The uptake of [1,2,3-^{3}H]-2-arachidonyl glycerol, (20–40 Ci·mmol^{-1}) in intact cells was performed using U937 cells. Briefly, 10^6 cells were re-suspended in 500 μL of serum-free medium in silanized plastic tubes and preincubated with different concentrations of α-amyrin, β-amyrin or JZL184 for 30 min at 37°C. Then, a mixture of 2-AG/[^{3}H]-2-AG to a final concentration of 1 μM, was added to the cells and incubated for 5 min at 37°C. The uptake process was stopped by placing the tubes on ice and rapidly centrifuging them at 800 × *g* for 5 min at 4°C. The supernatant was collected and transferred into 1 mL of a methanol : chloroform mixture 1:1 (v/v), while the pellet was re-suspended in ice-cold PBS plus 1% of fatty acid-free BSA and centrifuged at 800 × *g* for 5 min at 4°C (washing step). The washing solution was discarded while the cell pellet was re-suspended in 250 μL of ice-cold PBS and transferred into 500 μL of a methanol : chloroform mixture 1:1 (v/v), vortexed vigorously, sonicated on ice-cold water bath for 5 min and finally centrifuged at 10 000 × *g* for 10 min at 4°C. The aqueous phase was pooled with the aqueous phase extracted from the supernatant and transferred in a scintillation tube while the lipophilic phase was transferred in a separated tube. The radioactivity associated with the intracellular [^{3}H]-2-AG or the hydrolysis product [^{3}H]-glycerol was measured by adding 3 mL of Ultima Gold scintillation liquid (PerkinElmer Life Sciences) using a Tri-Carb 2100 TR scintillation counter (PerkinElmer Life Sciences). Data were collected from three independent experiments each performed in triplicates. Results were expressed as [^{3}H]-glycerol formation (or [^{3}H]-2-AG intracellular accumulation), relative to that in vehicle-treated samples (=100%).

Quantification of AEA and 2-AG levels by GC-MS

The quantification of the endogenous AEA and 2-AG level was performed according to a published method (Marazzi *et al.*, 2011). Briefly, 2.5 mL of diluted pig brain homogenate in 10 mM Tris-HCl and 1 mM EDTA, pH 7.6 (corresponding to 1.8 mg of protein) was incubated with α-amyrin, β-amyrin, PMSF or JZL184 for 30 min at 37°C with shaking. After incubation, lipids were extracted by Folch extraction (Folch *et al.*, 1957), transferring the brain homogenate to 15 mL of ice-cold chloroform/methanol 2:1 containing internal standards (the final mixture was 4:2:1 /$CHCl_3$: CH_3OH : H_2O, v/v/v). The suspension was vortexed vigorously, sonicated for 5 min on ice-cold water bath and centrifuged for 10 min at 500 × *g*. The organic phase was transferred to a glass vial, dried under N_2, reconstituted in 1 mL ethanol, diluted with 9 mL of water and finally extracted by solid-phase extraction with C-18 Sep-Pak cartridge (Waters AG, Zug, Switzerland). The internal standards used for the quantification were: *N*-arachidonoylethanolamine-d4 1 ng·μL^{-1} (25 ng per sample), 2-arachidonoylglycerol-d5 8 ng·μL^{-1} (200 ng per sample). Derivatization of the hydroxyl groups was performed with the silylating agent dimethylisopropylsilyl imidazole at room temperature for 1 h as previously reported (Obata *et al.*, 2003). The samples were analysed by GC-electron ionization (EI)-MS using an Agilent 6890 N GC equipped with a 30 m HP-5MS column and a 5975 C EI-MS with triple-axis detector. Helium was used as carrier gas at a constant flow rate of 1.5 mL·min^{-1} with splitless injection at an inlet temperature of 250°C. Optimal separation of the analytes was achieved with the following oven programme: initial temperature of 150°C for 1 min, followed by an increase to 280°C at 8°C·min^{-1} with a final time of 20 min. Because of acyl group migration of 2-AG during lipid extraction and purification, a significant amount of 1-AG was formed. Therefore, the peak areas of 1-AG and 2-AG were combined for all quantifications.

Data analysis

Results are expressed as mean values ± SEM for each examined group. Statistical significance of differences between groups was determined by the Student's *t*-test (paired *t*-test) with GraphPad Prism 5 software (GraphPad Software Inc., San Diego, CA, USA). Outliers in a series of identical experiments were determined by Grubb's test (ESD method) with α set to 0.05. Statistical differences between treated and vehicle control groups were determined by Student's *t*-test for dependent samples. Differences between the analysed samples were considered as significant if $P \leq 0.05$.

Materials

[Ethanolamine-1-^{3}H]-anandamide (^{3}H-AEA) (40–60 Ci·mmol^{-1}) and [1,2,3-^{3}H]-2-arachidonyl glycerol (20–40 Ci·mmol^{-1}) were obtained from American Radiolabeled Chemicals Inc. (Saint Louis, MO, USA), and the radioligand [^{3}H]-CP-55 940 (168 Ci·mmol^{-1}) was obtained from PerkinElmer Life Sciences (Waltham, MA, USA). WIN55,212-2, AEA, 2-arachidonoyl glycerol (2-AG), JZL184, WWL70 and tetrahydrolipstatin (THL) were obtained from Cayman Chemicals Europe (Tallin, Estonia). Pristimerin and α-amyrin were purchased from Fluka Sigma-Aldrich (Buchs, Switzerland) while the structural isomer β-amyrin (~95%) was kindly provided by Professor Dr. Giovanni Appendino. The natural products α-amyrin and β-amyrin were also purchased from Extrasynthese (Lyon, France) with a purity of ≥98.0%. Purity in stock solutions was checked by GC-MS. In the experiments, all batches were used to rule out differences between different sources.

Results

First, the two structural isomers of amyrin (Figure 1) were tested in radioligand binding assays for both cannabinoid

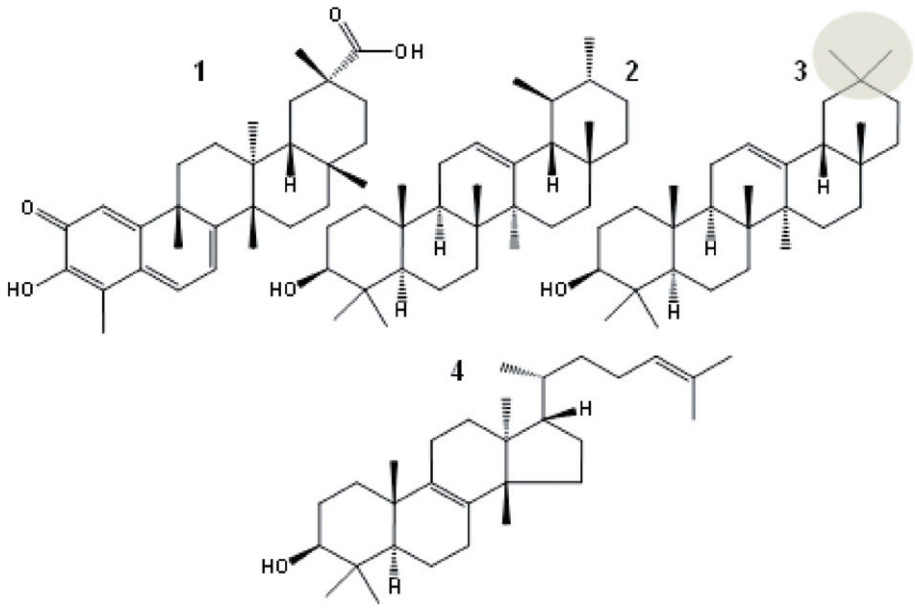

Figure 1

Chemical structures of the triterpenes pristimerin (1), α-amyrin (2), β-amyrin (3) and euphol (4), all of which inhibit 2-AG hydrolysis. β-Amyrin (3) with geminal methyl groups in ring A (grey circle) is the most effective inhibitor of 2-AG degradation in cellular extracts.

receptors using membrane preparations obtained from CHO-K1 cells stably transfected with *h*CB_1 or *h*CB_2 receptors, respectively. β-Amyrin induced only a slight partial displacement of the radioligand from CB_1 receptors at 1 μM (approximately 25%), while α-amyrin inhibited radioligand binding at concentrations ≥10 μM (Figure 2A). As shown in Figure 2B, both α- and β-amyrin did not strongly displace [^{3}H]-CP55940 from CB_2 receptors at concentrations below 10 μM. Thus, in our hands, α- and β-amyrin are not or are very weak CB_1 receptor ligands. Because the study by da Silva *et al*. (2011) showed a very consistent CB receptor-dependent antinociceptive effect *in vivo*, we tested whether amyrins interact with other major components of the endocannabinoid system. We used two different methods to address potential effects on AEA and 2-AG hydrolysis: the classical radioactivity-based assays using [^{3}H]-AEA and [^{3}H]-2-AG and absolute GC-MS quantification of the endogenous endocannabinoid levels in brain homogenate. Both α- and β-amyrin were assessed for FAAH activity in the concentration range of 0.1 nM–10 μM and the results obtained by both methods showed no inhibition of AEA hydrolysis (Figure 3). PMSF was used as positive control showing a complete reduction of [^{3}H]-ethanolamine formation in radioactivity experiments, as well as an accumulation of the endogenous AEA in the pig brain homogenate (Figure 3). Next, we evaluated the effects of α- and β-amyrin on 2-AG hydrolysis in the same homogenate. As shown in Figure 4, β-amyrin exhibited a concentration-dependent reduction of [^{3}H]-glycerol formation starting at 10 nM and reaching the maximal effect of 35–40% inhibition at 10 μM. Likewise, α-amyrin led to a slight (about 5–8%), but significant 2-AG hydrolysis inhibition at 10 nM, but reaching only 20% of the maximal inhibition effect at 10 μM (Figure 4A). In the same system, JZL184 was used as a positive control for the inhibition of MAGL, the main enzyme involved in 2-AG hydrolysis in the brain (Labar *et al*., 2010; Lichtman *et al*., 2010). The concentration–inhibition curves of JZL184 and β-amyrin showed a similar trend without major differences in maximal inhibition at 10 μM. A further positive control included 1 μM of JZL184 in combination with 10 μM of WWL70 and 20 μM of THL [inhibitors of ABHD-6 and –12, respectively, two enzymes recently identified to hydrolyse 2-AG in the brain (Blankman *et al*., 2007; Marrs *et al*., 2010)]. This combination reduced [^{3}H]-glycerol formation to 20% of vehicle control, confirming that MAGL, unlike FAAH for AEA, is not the only enzyme involved in 2-AG hydrolysis in the brain. Thus, β-amyrin inhibited 2-AG hydrolysis in a concentration-dependent manner, similar to that of JZL184, although not reaching the same maximal inhibition in pig brain homogenates.

To further investigate the inhibition of 2-AG hydrolysis by the amyrins in a more physiological setting, we incubated pig brain homogenates with amyrins, JZL184, or vehicle at 37°C for 30 min without adding any 2-AG and then quantified the endocannabinoid levels by GC-MS. As shown in Figure 4B, β-amyrin led to a significant inhibition of endogenous 2-AG hydrolysis, as shown by the increased 2-AG levels (140 and 240% at 1 and 10 μM, respectively). Similarly, JZL184 treatment produced an increase of 2-AG levels of 240 and 300% at 1 and 10 μM, respectively. Unlike the experiments with radiolabelled substrate, in this more complex homogenate, neither β-amyrin nor JZL184 produced a significant inhibition of 2-AG hydrolysis at 100 nM (Figure 4B). This may be due to the higher detection limit for endogenous 2-AG compared with radioactive assays. In keeping with this hypothesis, α-amyrin did not show any significant accumulation of endogenous 2-AG up to 10 μM, while a slight, but significant reduction of [^{3}H]-glycerol formation was observed in the radioactive experiments (Figure 4B).

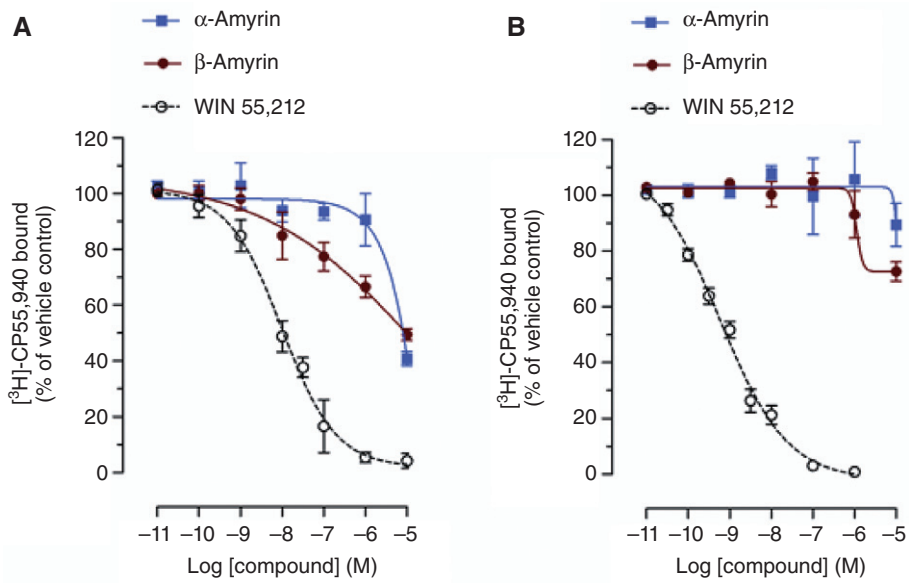

Figure 2

Radioligand binding assay using CHO-K1 cells stably transfected with (A) hCB_1 and (B) hCB_2 receptors and 0.5 nM [^{3}H]-CP55,940. The potent non-specific CB receptor ligand WIN55,212-2 was used as a positive control. Although β-amyrin displaced ~30% at 1 μM of [^{3}H]-CP55,940 at the CB_1 receptor, no IC_{50} was reached at concentrations <10 μM. A racemic α,β-amyrin 1:1 mixture was assessed at 10 μM and did not exhibit significantly higher [^{3}H]-CP55,940 displacement than the isomers tested separately (data not shown). Data show means ± SEM, $n = 12$ from four independent experiments.

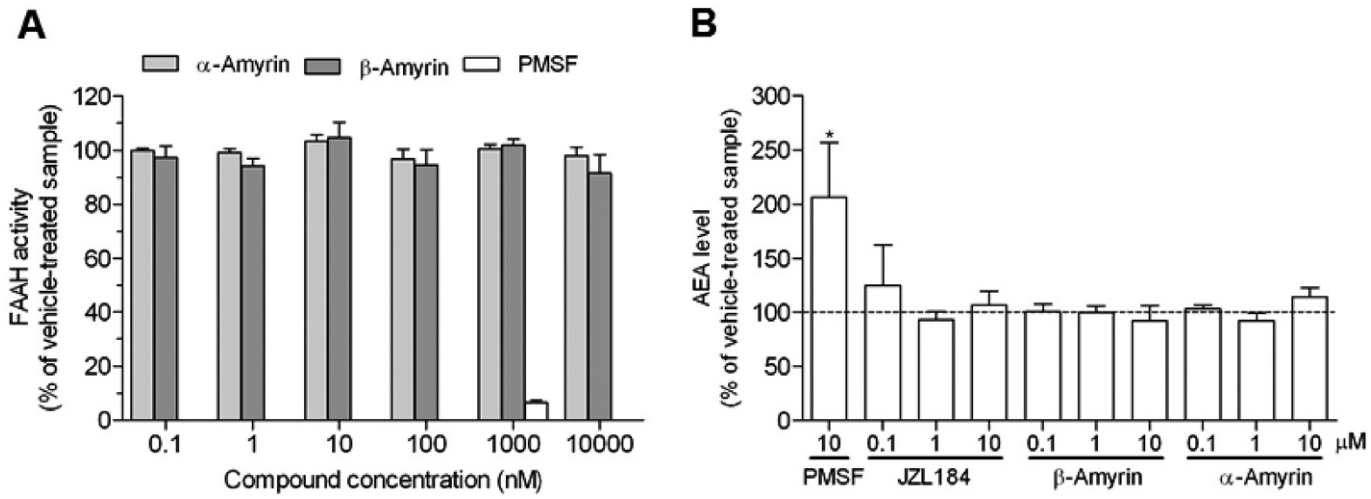

Figure 3

Neither α- nor β-amyrin show inhibition of AEA hydrolysis. (A) FAAH activity was measured by incubating 200 μg of pig brain homogenate with 2 μM of the AEA/[^{3}H]-AEA mixture for 10 min at 37°C after 20 min preincubation with amyrins, PMSF or vehicle. (B) Absolute quantification of the AEA level by GC-MS in 1.8 mg pig brain homogenate after 30 min incubation at 37°C with amyrins, PMSF or vehicle. Data show means ± SEM of nine measurements from three independent experiments. *$P < 0.05$, significantly different from vehicle-treated samples.

The results obtained showed significant inhibition of 2-AG hydrolysis by β-amyrin *in vitro*. Therefore, we further investigated whether this molecule could interact with 2-AG trafficking and degradation in cells. We assessed the intracellular accumulation of [^{3}H]-2AG as well as the amount of [^{3}H]-glycerol formed in U937 cells. As expected for a 2-AG hydrolysis inhibitor, β-amyrin treatment resulted in a significant concentration-dependent increase of intracellular 2-AG compared with vehicle control in the nanomolar and sub-nanomolar concentrations (Figure 5A). Noteworthy, α-amyrin also induced a similar concentration-dependent 2-AG accumulation curve, but with lower efficacy than β-amyrin, in agreement with its weaker inhibition of 2-AG hydrolysis. The MAGL inhibitor JZL184, which was tested in

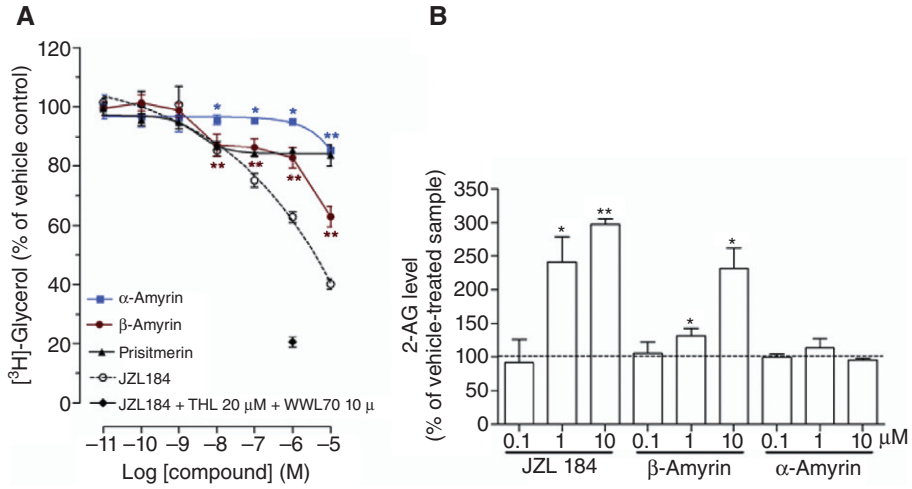

Figure 4

Inhibition of 2-AG hydrolysis by amyrins. (A) Dose-dependent inhibition of [^{3}H]-glycerol formation in pig brain homogenate after 30 min pretreatment with amyrins, JZL184, JZL184 1 μM + 10 μM WWL70 + 20 μM THL or vehicle, followed by 10 min incubation at 37°C with 10 μM of the 2-AG/[^{3}H]-2-AG mix. (B) Absolute quantification of the 2-AG level by GC-MS in 1.8 mg pig brain homogenate after 30 min incubation with amyrins, JZL184 or vehicle at 37°C. Data show means ± SEM, $n = 9$ from three independent experiments. *$P < 0.05$, **$P < 0.01$, significantly different from vehicle-treated samples (=100%).

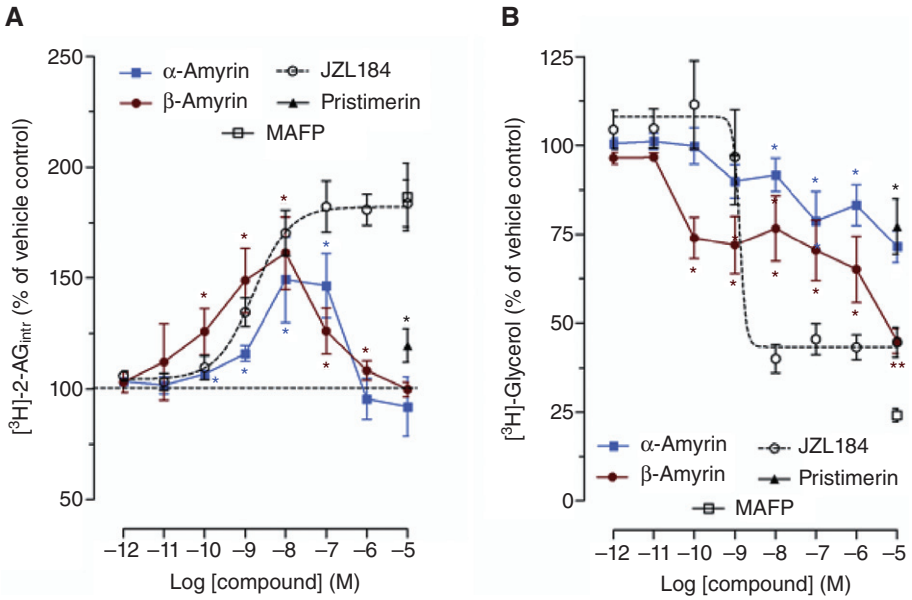

Figure 5

The effect of amyrins on 2-AG trafficking and breakdown in intact U937 cells. (A) [^{3}H]-2-AG intracellular levels and (B) [^{3}H]-glycerol formation in U937 cells pretreated with amyrins, JZL184 or vehicle and then incubated with 1 μM 2-AG/[^{3}H]2-AG mix for 5 min. The effect of pristimerin and MAFP is shown only at a concentration of 10 μM. The radioactive counts in the vehicle controls were approximately 9000 and 300 dpm for [^{3}H]-glycerol formation and intracellular [^{3}H]-2-AG, respectively. Data show means ± SEM, $n = 9$ from three independent experiments. *$P < 0.05$, **$P < 0.01$, significantly different from vehicle-treated samples (=100%).

the same conditions, led to a curve identical to that of β-amyrin in the nanomolar concentrations, further supporting MAGL inhibition by the triterpene. Interestingly, unlike JZL184, both α- and β-amyrin at higher concentrations (1 and 10 μM) partially or completely lost the ability to increase intracellular accumulation of 2-AG, but without altering the inhibition of [^{3}H]-glycerol formation (Figure 5A and B). In fact, the two structural isomers inhibited [^{3}H]-glycerol formation in a concentration-dependent manner up to 10 μM without losing efficacy. In agreement with our 2-AG

hydrolysis experiments, β-amyrin was more potent than α-amyrin (Figure 5B). As an additional positive control, we tested the triterpene pristimerin, which is a reversible inhibitor of MAGL (King *et al.*, 2009a). The effect of the non-selective inhibitor of hydrolases, methoxy arachidonyl fluorophosphonate (MAFP), was also measured in the [^{3}H]-2-AG uptake assay. 10 μM of MAFP led to the same intracellular [^{3}H]-2-AG accumulation as the maximal effect obtained with JZL184 (approximately 200%) (Figure 5A). In contrast, MAFP treatment led to a stronger inhibition than JZL184 of the [^{3}H]-glycerol production (75 and 55%, respectively) (Figure 5B). The latter difference can be explained by the broader spectrum of hydrolase inhibition by MAFP at 10 μM, which *in vitro* was shown to fully inhibit MAGL and FAAH and, at least partially, also ABHD-6 and ABHD-12 (Hoover *et al.*, 2008). In the same [^{3}H]-2-AG uptake assay, we also assessed the effect of the triterpene MAGL inhibitor pristimerin. As shown in Figure 5, 10 μM pristimerin produced a 25% inhibition of [^{3}H]-glycerol formation and a 125% accumulation of intracellular [^{3}H]-2-AG, thus being less potent than β-amyrin in this assay.

The unexpected reduction of [^{3}H]-2-AG accumulation by the amyrins at higher concentrations (Figure 5A) could be the result of 'off-target' effects such as, for example an interaction with a putative 2-AG membrane transporter. In order to address this hypothesis, we measured the effect of α- and β-amyrin on [^{3}H]-2-AG uptake and degradation in U937 cells in presence of MAGL inhibition by 10 μM JZL184, which does not affect 2-AG uptake (Fowler and Ghafouri, 2008). The data indicate that at low concentrations (0.1–1 nM), β-amyrin still led to a slight but significant increase of intracellular [^{3}H]-2-AG (10–20%) over the 10 μM JZL184-treated cells, while at higher concentrations (0.1–10 μM) a significant decrease of the intracellular [^{3}H]-2-AG (25–40%) as compared with JZL184-treated cells is shown (Figure 6A). Similarly, U937 cells treated with α-amyrin in the presence of 10 μM JZL184 did not accumulate intracellular [^{3}H]-2-AG at low concentrations, whereas at higher concentrations, a reduction of [^{3}H]-2-AG uptake (10–25%) was observed (Figure 6B). As shown in Supporting Information Figure S1, inhibition of [^{3}H]-glycerol formation via [^{3}H]-2-AG hydrolysis was independent of JZL184 treatment. This suggests that the reduction of [^{3}H]-glycerol formation is dependent on inhibition of both 2-AG hydrolysis and cellular uptake. Intriguingly, at 0.1 nM β-amyrin, [^{3}H]-glycerol formation was significantly inhibited, compared with that in cells treated with JZL184 (10 μM). This clearly suggested an additional 2-AG hydrolysis inhibition independent of MAGL. On the basis of this potential non-MAGL-mediated inhibition of 2-AG hydrolysis, we measured the MAGL and non-MAGL components by using purified *h*MAGL and mouse microglial BV2 cells, which lack MAGL, but still retain 2-AG hydrolysis via ABHDs [mainly ABHD-6 (Marrs *et al.*, 2010)]. As shown in Figure 7A, β-amyrin inhibited purified *h*MAGL more potently than α-amyrin (see IC_{50} values in Table 1). Pristimerin and JZL184 produced a total inhibition of MAGL (Figure 7A), with IC_{50} values (Table 1), in concordance with published values (King *et al.*, 2009a; Long *et al.*, 2009). As shown in Figure 7B, in BV2 cell homogenates, α- and β-amyrin induced a partial but significant inhibition (10–20%) of [^{3}H]-2-AG hydrolysis at concentrations ≥100 nM indicating additional non-MAGL targets. Importantly, JZL184 did not inhibit [^{3}H]-2-AG hydrolysis in this system below 10 μM, which is in agreement with its selectivity towards MAGL (Long *et al.*, 2009). The triterpene pristimerin only produced a very weak partial inhibition (<10%) at 10 μM, reflecting its MAGL selectivity (Figure 7B). The assay was validated using the ABHD-6 inhibitor WWL70, which showed an almost complete inhibition of [^{3}H]-2-AG hydrolysis (75–80%) at 10 μM (Figure 7B).

Our data showed that β-amyrin exerts a significant mixed action on enzymes hydrolysing 2-AG, targeting MAGL and ABHDs. Becauase MAGL is the main enzyme involved in

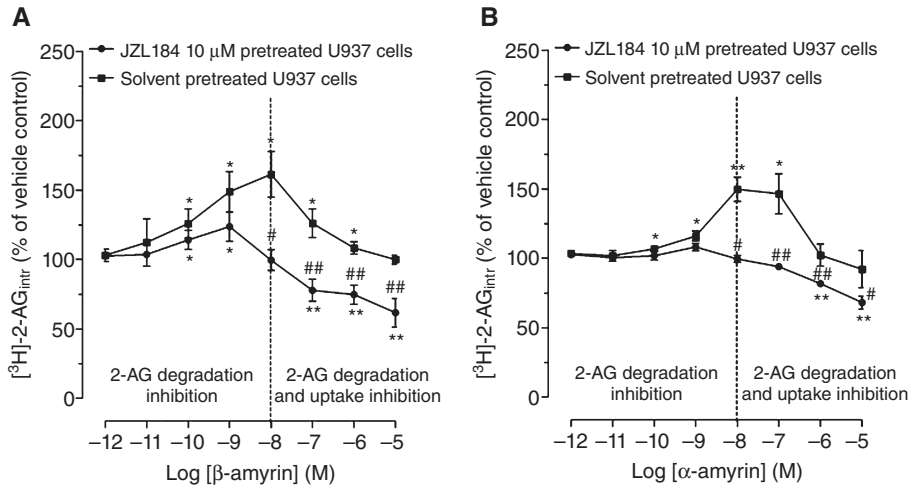

Figure 6

The effect of amyrins on 2-AG uptake in intact U937 cells pretreated with 10 μM JZL184. Intracellular [^{3}H]-2-AG levels in U937 cells pretreated with (A) β-amyrin plus JZL184 or β-amyrin plus vehicle, (B) α-amyrin plus JZL184 or α-amyrin plus vehicle incubated with 1 μM 2-AG/[^{3}H]-2-AG for 5 min. Data show mean values ± SEM, $n = 12$ from four independent experiments. *$P < 0.05$, **$P < 0.01$, significantly different from vehicle control (=100%). #$P < 0.05$, ##$P < 0.01$, JZL184 plus amyrin-treated cells significantly different from amyrin-treated cells (=100%).

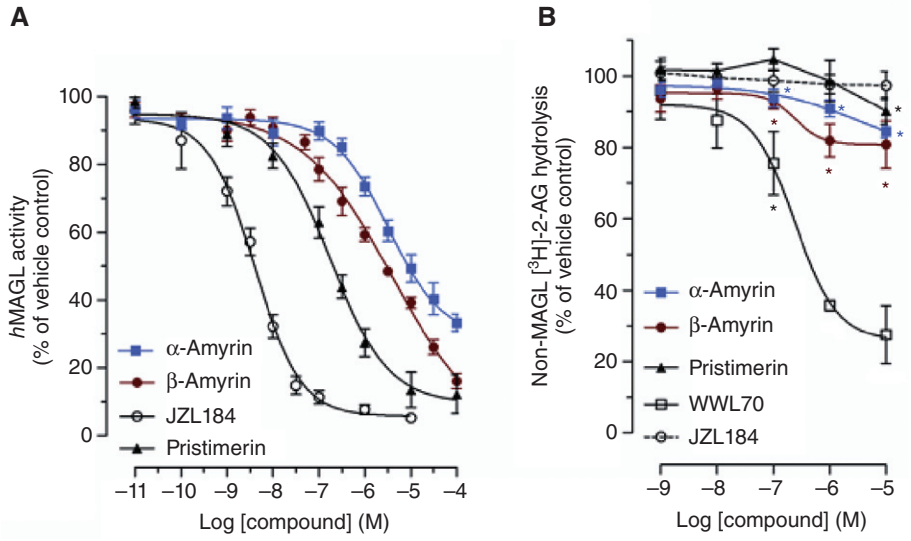

Figure 7

MAGL and non-MAGL components in the inhibition of 2-AG hydrolysis by α- and β-amyrin. (A) Concentration-dependent inhibition of purified *h*MAGL activity by α-amyrin, β-amyrin, pristimerin and JZL184. (B) Concentration-dependent inhibition of [^{3}H]-2-AG hydrolysis in BV2 cell homogenate in presence of 1 μM URB597 and different concentrations of α-amyrin, β-amyrin, pristimerin, WWL70 and JZL184. Data show mean values ± SEM, $n = 12$ from four independent experiments. *$P < 0.05$, **$P < 0.01$ significantly different from vehicle control (=100%).

Table 1

IC_{50} values of amyrins, pristimerin and JZL184 calculated from the *h*MAGL inhibition curves

Compound	IC_{50} (nM) values ± SEM
α-Amyrin	9300 ± 1200
β-Amyrin	2800 ± 500
Pristimerin	204 ± 16.2
JZL184	3.9 ± 1.0

2-AG hydrolysis (Blankman *et al.*, 2007) we next assessed the mechanism of action of β-amyrin towards MAGL. As shown in Figure 8A, 3 μM of β-amyrin produced a rapid (1 min) and continuous inhibition of MAGL activity. In Figure 8B, we show the interaction of β-amyrin with purified *h*MAGL using a rapid dilution assay (King *et al.*, 2009b). Under these conditions, the incubation of MAGL with the covalent inhibitor MAFP resulted in the formation of an enzyme-inhibitor complex that was resistant to dilution of the assay mixture. By contrast, rapid dilution of the MAGL-β-amyrin mixture resulted in an almost full recovery of the enzymatic activity, suggesting a reversible inhibition. In Figure 8C, further kinetic studies demonstrated that β-amyrin decreased the maximal catalytic velocity (V_{max} in pmol·min·μg^{-1}) of MAGL from 43.9 ± 8.6 (vehicle) to 24.3 ± 4.6 (3 μM β-amyrin) without influencing its Michaelis–Menten constant (K_m: 1.31 ± 0.98 μM for the vehicle and 1.19 ± 0.67 μM for 3 μM β-amyrin). Together, these data show that β-amyrin inhibited MAGL activity in a rapid, reversible and non-competitive manner, similar to that previously shown for the structurally related, but more potent triterpene pristimerin (King *et al.*, 2009a).

Discussion and conclusions

Although we cannot fully explain the discrepancy between the ultrapotent CB_1 receptor interaction of α/β-amyrin reported (Da Silva *et al.*, 2011) and the lack of CB_1 receptor interaction in this study, it is likely to be related to methodology. Da Silva *et al.* used membranes prepared from rat brain (containing CB_1 receptors) or rat spleen (containing CB_2 receptors). The view that these tissues express either CB_1 or CB_2 receptors, respectively, is too simple as brain tissues are known to also contain CB_2 receptors (Onaivi, 2011) and spleen contains CB_1 receptors (Noe *et al.*, 2001). Moreover, in their study, the radioligands [^{3}H]-SR141716A (rimonabant) and [^{3}H]-CP55,940 were used, which both potentially interact with other targets in these tissues; for example SR141716A may directly interact with $GABA_A$ and GPR55 receptors (Anavi-Goffer *et al.*, 2011; Baur *et al.*, 2011). Notably, the binding curves published for α/β-amyrin were not sigmoidal, but were rather linear and only the specific binding was indicated whereas the actual binding (including % non-specific binding) was not shown (Da Silva *et al.*, 2011). In addition, we could also speculate that the CB_1 receptor binding of the inverse agonist [^{3}H]-SR141617A might be affected by amyrins via some unidentified interactions at different receptor sites. Thus, potential methodological issues cannot be excluded. Although we did not use rat, but human cannabinoid receptors, it is unlikely that the discrepancy was only due to species differences. We used an established and validated CB receptor binding assay (Gertsch *et al.*, 2008) and

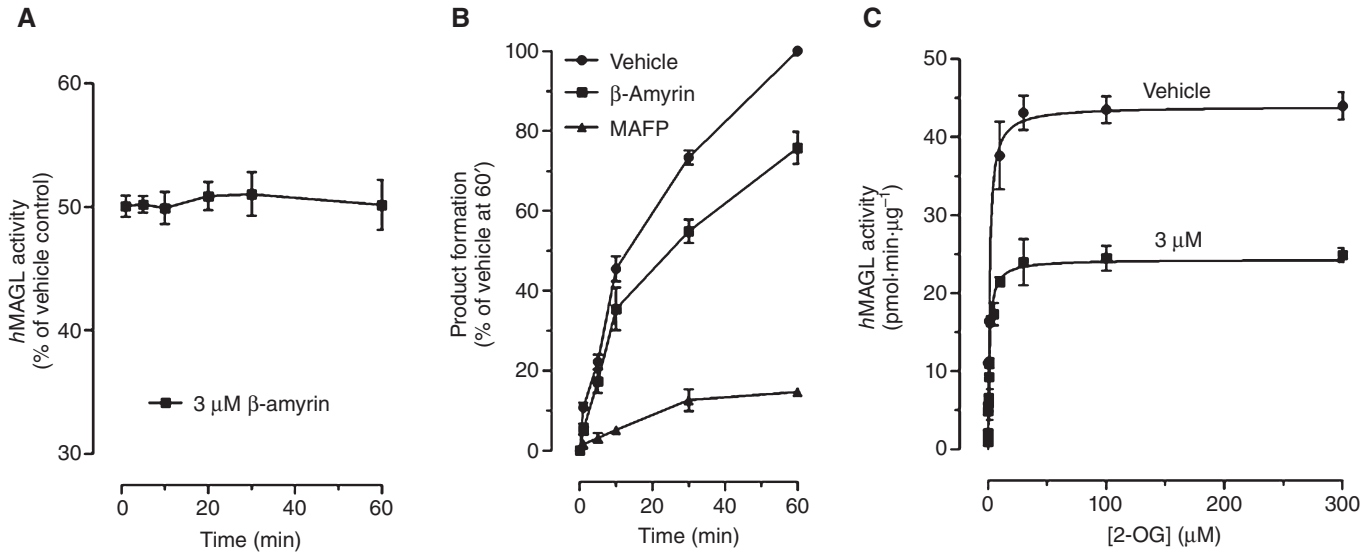

Figure 8

Mechanism of action of β-amyrin-mediated MAGL inhibition. (A) Time course of MAGL inhibition by 3 μM β-amyrin. (B) Rapid dilution assays of MAGL in the presence of vehicle, β-amyrin or MAFP. Results are expressed as percentage of product generated after 60 min incubation with vehicle. (C) Michaelis–Menten analysis of the MAGL reaction (measured as pmol·min^{-1}·μg protein^{-1}) in the presence of vehicle or 3 μM of β-amyrin. Data show mean values ± SEM, n = 9 from three independent experiments.

our positive control WIN55,212-2 showed a K_i value in the concentration range reported previously (McPartland *et al.*, 2007). Using our experimental system, we were unable to detect significant CB receptor binding in independent experiments.

In a profiling of α-amyrin and β-amyrin on other targets within the endocannabinoid system (endocannabinoid transport across membranes and hydrolytic degradation), we found significant inhibitory effects on 2-AG hydrolysis by amyrins. The geminal methyls (β-amyrin) in the A ring were more effective than the vicinal methyl groups (α-amyrin). The finding that β-amyrin inhibits 2-AG hydrolysis in different biological preparations may also explain the CB_1 receptor binding of β-amyrin reported by da Silva *et al*. The brain homogenate used for CB_1 receptor binding may lead to a significant rise of background 2-AG levels (Sugiura *et al.*, 2001), which is the most abundant endocannabinoid in the brain, and could thus interfere with the relative [^{3}H]-SR141716A binding. In fact, rat brain membranes retain some 2-AG hydrolytic enzymes such as ABHDs, which are integral cell membrane proteins (Blankman *et al.*, 2007; Ahn *et al.*, 2008), and MAGL, which is found associated with the inner cell membrane leaflet (Labar *et al.*, 2010). Indeed, da Silva *et al*. reports that rats were killed by decapitation before preparing the brain membranes (Da Silva *et al.*, 2011). This procedure has been shown to produce a strong accumulation of 2-AG in the rat brain to up to 1.54 nmol g^{-1} of tissue 30 s after decapitation (Sugiura *et al.*, 2001), thus leading to even a higher 2-AG content in the membrane preparations used for the CB_1 receptor binding assay. That the inhibition of 2-AG breakdown in rat brain homogenates was able to interfere with [^{3}H]-SR141716A binding cannot be excluded at this point. In the paper by da Silva *et al.*, pre-incubation of the rat brain membranes before adding the amyrins could have removed the residual 2-AG through the action of the retained hydrolytic activity.

Pristimerin, another structurally related pentacyclic triterpenoid is a potent reversible inhibitor of MAGL activity (King *et al.*, 2009a), which is in agreement with our finding that amyrin inhibits 2-AG breakdown. In our hands, pristimerin was less potent in inhibiting 2-AG breakdown than β-amyrin in brain tissue, despite the fact that in purified enzyme assays, pristimerin was an approximately 10-fold more potent inhibitor of *h*MAGL (Table 1 and Figure 7A). This could be explained by the fact that the amyrins, but not pristimerin, also inhibit ABHDs, as shown in the experiments using BV2 cell homogenates where MAGL is not expressed (Marrs *et al.*, 2010). Thus, relatively weak and partial simultaneous inhibition of MAGL and ABHDs appears to be synergistic, leading to significant pharmacological inhibition of 2-AG metabolism. That triterpenoids may be a yet unexploited source for MAGL inhibitors is also shown by euphol, which is a different plant tetracyclic terpene that has been reported to inhibit MAGL, albeit less potently than pristimerin (King *et al.*, 2009a). Interestingly, Dutra *et al*. from the same laboratory in which α/β-amyrin was found to be an ultrapotent CB_1 receptor ligand recently reported that the triterpene euphol is an ultrapotent CB_2 receptor-selective agonist with a subnanomolar K_i value (Dutra *et al.*, 2011). In this study again rat spleen was used and no functional data were reported. As observed with α/β-amyrin, the antinociceptive effects (neuropathic pain model) of euphol could be inhibited by both CB_1 and CB_2 receptor antagonists, pointing to an indirect cannabimimetic effect via the previously described inhibition of MAGL by euphol (King *et al.*, 2009a). In our ongoing CB receptor screening activities using natural product libraries (Gertsch *et al.*, 2006; 2010; Leonti *et al.*, 2010), we have so far not found any triterpenoid with significant CB receptor affinity towards the classical

CP55,940 binding site (i.e. targeting the endocannabinoid binding pocket). However, a sulphur containing steroid with a triterpenoid-like steroid scaffold from a marine sponge was recently reported to selectively bind to the CB_2 receptor with a K_i value at low micromolar concentrations (Chianese *et al.*, 2011). Nevertheless, CB receptor ligands from steroids or triterpenes are generally lacking. Overall, plant triterpenoids, many of which are found in medicinal plants and known to exert significant anti-inflammatory and antinociceptive effects (Ríos, 2010), appear to offer a very broad and largely unexplored scaffold for potent inhibitors of 2-AG metabolism by non-selectively targeting MAGL and ABHDs. Future studies will address this hypothesis.

A recent study reported the pharmacokinetic profile of amyrin in rats (Ching *et al.*, 2011). In this study, the absolute oral bioavailability of *β*-amyrin was in the range of 0.8–3.8%, depending on purity and admixtures. Although only partly bioavailable, *β*-amyrin showed a very long terminal elimination half-life ($t1/2\lambda z$ = 610 ± 179 min) and extremely slow clearance (Cl = 2.04 ± 0.24 mL·min·kg^{-1}) (Ching *et al.*, 2011). The data by da Silva *et al.* suggest that ~0.3 mg kg^{-1} of bioavailable α/*β*-amyrin from a total of 30 mg·kg^{-1} orally administered dose is enough to exert significant *in vivo* effects when administered chronically, indicating either tissue accumulation (depot effect) or high potency. Of note, the specific MAGL inhibitor JZL184 is only poorly orally bioavailable (unpublished data) and triterpenoid MAGL/ABHDs inhibitors like β-amyrin may thus provide novel tool compounds. Because β-amyrin is a widespread constituent of many anti-inflammatory medicinal plants and vegetable foods, MAGL inhibition could contribute to the network pharmacology exerted by anti-inflammatory botanical drugs (Gertsch, 2011). Given that Nature produces a wide variety of distinct tetracyclic and pentacyclic terpenes, their potential effects on MAGL need to be addressed systematically in future studies.

Acknowledgements

This work was supported by the Swiss National Science Foundation NCCR TransCure and the by the Novartis Research Foundation grant 10B48. The study was within the framework of the COST action Chemical Biology with Natural Products. We would like to thank Giovanni Appendino, Università degli Studi del Piemonte Orientale, for kindly providing β-amyrin. Some AEA transport assays that are not shown were performed by Simon Nicolussi in our laboratory.

Conflict of interest

The authors state no conflicts of interest.

References

Ahn K, McKinney MK, Cravatt BF (2008). Enzymatic pathways that regulate endocannabinoid signaling in the nervous system. Chem Rev 108: 1687–1707.

Akihisa T, Yasukawa K, Oinuma H, Kasahara Y, Yamanouchi S, Takido M *et al.* (1996). Triterpene alcohols from the flowers of compositae and their anti-inflammatory effects. Phytochemistry 43: 1255–1260.

Alexander SP, Mathie A, Peters JA (2011). Guide to Receptors and Channels (GRAC), 5th edition. Br J Pharmacol 164: S1–S324.

Anavi-Goffer S, Baillie G, Irving AJ, Gertsch J, Greig IR, Pertwee RG *et al.* (2011). Modulation of L-α-lysophosphatidylinositol/GPR55 MAP kinase signalling by cannabinoids. J Biol Chem 287: 91–104.

Baur R, Gertsch J, Sigel E (2011). The cannabinoid receptor CB1 antagonists rimonabant (SR141716) and AM251 directly potentiate GABA(A) receptors. Br J Pharmacol 165: 2479–2484.

Bisogno T, Di Marzo V (2010). Cannabinoid receptors and endocannabinoids: role in neuroinflammatory and neurodegenerative disorders. CNS Neurol Disord Drug Targets 5: 564–573.

Björklund E, Noren E, Nilsson J, Fowler CJ (2010). Inhibition of monoacylglycerol lipase by troglitazone, N-arachidonoyldopamine and the irreversible inhibitor JZL184: comparison of two different assays. Br J Pharmacol 161: 1512–1526.

Blankman JL, Simon GM, Cravatt BF (2007). A comprehensive profile of brain enzymes that hydrolyze the endocannabinoid 2-arachidonoylglycerol. Chem Biol 14: 1347–1356.

Breivogel C (2006). Cannabinoid receptor binding to membrane homogenates and cannabinoid-stimulated [35S]GTP-S binding to membrane homogenates or intact cultured cells. Marijuana and cannabinoid research. Methods Mol Med 123: 149–162.

Chianese G, Fattorusso E, Taglialatela-Scafati O, Bavestrello G, Calcinai B, Dien HA *et al.* (2011). Desulfohaplosamate, a new phosphate-containing steroid from Dasychalina sp., is a selective cannabinoid CB2 receptor ligand. Steroids 76: 998–1002.

Chicca A, Raduner S, Pellati F, Strompen T, Altmann KH, Schoop R *et al.* (2009). Synergistic immunomopharmacological effects of N-alkylamides in Echinacea purpurea herbal extracts. Int Immunopharmacol 9: 850–858.

Ching J, Lin HS, Tan CH, Koh HL (2011). Quantification of α- and β-amyrin in rat plasma by gas chromatography-mass spectrometry: application to preclinical pharmacokinetic study. J Mass Spectrom 46: 457–464.

Da Silva KA, Paszcuk AF, Passos GF, Silva ES, Bento AF, Meotti FC *et al.* (2011). Activation of cannabinoid receptors by the pentacyclic triterpene α,β-amyrin inhibits inflammatory and neuropathic persistent pain in mice. Pain 152: 1872–1287.

Dutra RR, Silva KB, Bento AF, Paszcuk AF, Marcon R, Meiotti FC *et al.* (2011). Euphol, a novel cannabinoid agonist, prevents inflammatory and neuropathic persistent pain in rodents. Planta Med 77: 1254.

Folch J, Lees M, Sloane Stanley GH (1957). A simple method for the isolation and purification of total lipides from animal tissues. J Biol Chem 226: 497–509.

Fowler CJ, Ghafouri N (2008). Does the hydrolysis of 2-arachidonoylglycerol regulate its cellular uptake? Pharmacol Res 58: 72–76.

Fride E, Perchuk A, Hall FS, Uhl GR, Onaivi ES (2006). Behavioural methods in cannabinoid research. Methods Mol Med 123: 269–290.

Gertsch J (2011). Botanical drugs, synergy, and network pharmacology: forth and back to intelligent mixtures. Planta Med 77: 1086–1098.

Gertsch J, Raduner S, Altmann KH (2006). New natural noncannabinoid ligands for cannabinoid type-2 (CB2) receptors. J Recept Signal Transduct Res 26: 709–730.

Gertsch J, Leonti M, Raduner S, Racz I, Chen JZ, Xie XQ *et al.* (2008). A. Beta-caryophyllene is a dietary cannabinoid. Proc Natl Acad Sci USA 105: 9099–90104.

Gertsch J, Pertwee RG, Di Marzo V (2010). Phytocannabinoids beyond the Cannabis plant – do they exist? Br J Pharmacol 160: 523–529.

Griffith DA, Hadcock JR, Black SC, Iredale PA, Carpino PA, DaSilva-Jardine P *et al.* (2009). Discovery of 1-[9-(4-chlorophenyl)-8-(2-chlorophenyl)-9H-purin-6-yl]-4-ethylaminopiperidine-4-carboxylic acid amide hydrochloride (CP-945,598), a novel, potent, and selective cannabinoid type 1 receptor antagonist. J Med Chem 52: 234–237.

Guindon J, Hohmann AG (2008). Cannabinoid CB2 receptors: a therapeutic target for the treatment of inflammatory and neuropathic pain. Br J Pharmacol 153: 319–334.

Hadcock JR, Carpino PA, Iredale PA, Dow RL, Gautreau D, Thiede L *et al.* (2010). Quantitative in vitro and in vivo pharmacological profile of CE-178253, a potent and selective cannabinoid type 1 (CB1) receptor antagonist. BMC Pharmacol 10: 9.

Holanda Pinto SA, Pinto LM, Guedes MA, Cunha GM, Chaves MH, Santos FA *et al.* (2008). Antinoceptive effect of triterpenoid alpha,beta-amyrin in rats on orofacial pain induced by formalin and capsaicin. Phytomedicine 15: 630–634.

Hoover HS, Blankman JL, Niessen S, Cravatt BF (2008). Selectivity of inhibitors of endocannabinoid biosynthesis evaluated by activity-based protein profiling. Bioorg Med Chem Lett 18: 5838–5841.

Huffman JW, Zengin G, Wu M, Lu J, Hynd G, Bushell K *et al.* (2005). Structure-activity relationships for 1-alkyl-3-(1-naphthoyl)indoles at the cannabinoid CB(1) and CB(2) receptors: steric and electronic effects of naphthoyl substituents. New highly selective CB(2) receptor agonists. Bioorg Med Chem 13: 89–112.

King AR, Duranti A, Tontini A, Rivara S, Rosengarth A, Clapper JR *et al.* (2007). URB602 inhibits monoacylglycerol lipase and selectively blocks 2-arachidonoylglycerol degradation in intact brain slices. Chem Biol 14: 1357–1365.

King AR, Dotsey EY, Lodola A, Jung KM, Ghomian A, Qiu Y *et al.* (2009a). Discovery of potent and reversible monoacylglycerol lipase inhibitors. Chem Biol 16: 1045–1052.

King AR, Lodola A, Carmi C, Fu J, Mor M, Piomelli D (2009b). A critical cysteine residue in monoacylglycerol lipase is targeted by a new class of isothiazolinone-based enzyme inhibitors. Br J Pharmacol 157: 974–983.

Labar G, Bauvois C, Borel F, Ferrer JL, Wouters J, Lambert DM (2010). Crystal structure of the human monoacylglycerol lipase, a key factor in endocannabinoid signaling. Chembiochem 11: 218–227.

Leonti M, Casu L, Raduner S, Cottiglia F, Floris C, Altmann KH *et al.* (2010). Falcarinol is a covalent cannabinoid CB1 receptor antagonist and induces pro-allergic effects in skin. Biochem Pharmacol 79: 1815–1826.

Lichtman AH, Blankman JL, Cravatt BF (2010). Endocannabinoid overload. Mol Pharmacol 78: 993–995.

Long JZ, Li W, Booker L, Burston JJ, Kinsey SG, Schlosburg JE *et al.* (2009). Selective blockade of 2-arachidonoylglycerol hydrolysis produces cannabinoid behavioral effects. Nat Chem Biol 5: 37–44.

McPartland JM, Glass M, Pertwee RG (2007). Meta-analysis of cannabinoid ligand binding affinity and receptor distribution: interspecies differences. Br J Pharmacol 152: 583–593.

Marazzi J, Kleyer J, Paredes JM, Gertsch J (2011). Endocannabinoid content in fetal bovine sera – unexpected effects on mononuclear cells and osteoclastogenesis. J Immunol Methods 373: 219–228.

Marrs WR, Blankman JL, Horne EA, Thomazeau A, Lin YH, Coy J *et al.* (2010). The serine hydrolase ABHD6 controls the accumulation and efficacy of 2-AG at cannabinoid receptors. Nat Neurosci 13: 951–957.

Melo CM, Carvalho KM, Neves JC, Morais TC, Rao VS, Santos FA *et al.* (2010). Alpha,beta-amyrin, a natural triterpenoid ameliorates L-arginine-induced acute pancreatitis in rats. World J Gastroenterol 16: 4272–4280.

Melo CM, Morais TC, Tomé AR, Brito GA, Chaves MH, Rao VS *et al.* (2011). Anti-inflammatory effect of α,β-amyrin, a triterpene from Protium heptaphyllum, on cerulein-induced acute pancreatitis in mice. Inflamm Res 60: 673–681.

Noe SN, Newton C, Widen R, Friedman H, Klein TW (2001). Modulation of CB1 mRNA upon activation of murine splenocytes. Adv Exp Med Bio l493: 215–221.

Obata T, Sakurai Y, Kase Y, Tanifuji Y, Horiguchi T (2003). Simultaneous determination of endocannabinoids (arachidonylethanolamide and 2-arachidonylglycerol) and isoprostane (8-epiprostaglandin F2alpha) by gas chromatography-mass spectrometry-selected ion monitoring for medical samples. J Chromatogr B Analyt Technol Biomed Life Sci 792: 131–140.

Onaivi ES (2011). Commentary: functional Neuronal CB2 Cannabinoid Receptors in the CNS. Curr Neuropharmacol 9: 205–208.

Pacher P, Bátkai S, Kunos G (2006). The endocannabinoid system as an emerging target of pharmacotherapy. Pharmacol Rev 58: 389–462.

Papahatjis DP, Kourouli T, Abadji V, Goutopoulos A, Makriyannis A (1998). Pharmacophoric requirements for cannabinoid side chains: multiple bond and C1′-substituted delta 8-tetrahydrocannabinols. J Med Chem 41: 1195–1200.

Pertwee RG (2009). Emerging strategies for exploiting cannabinoid receptor agonists as medicines. Br J Pharmacol 156: 397–411.

Pertwee RG, Howlett AC, Abood ME, Alexander SP, Di Marzo V, Elphick MR *et al.* (2010). International Union of Basic and Clinical Pharmacology. LXXIX. Cannabinoid receptors and their ligands: beyond CB1 and CB2. Pharmacol Rev 62: 588–631.

Raduner S, Majewska A, Chen JZ, Xie XQ, Hamon J, Faller B *et al.* (2006). Alkylamides from Echinacea are a new class of cannabinomimetics. Cannabinoid type 2 receptor-dependent and -independent immunomodulatory effects. J Biol Chem 281: 14192–14206.

Rees HH, Britton G, Goodwin TW (1968). The biosynthesis of beta-amyrin. Mechanism of squalene cyclization. Biochem J 106: 659–665.

Ríos JL (2010). Effects of triterpenes on the immune system. J Ethnopharmacol 128: 1–14.

Sugiura T, Yoshinaga N, Waku K (2001). Rapid generation of 2-arachidonoylglycerol, an endogenous cannabinoid receptor ligand, in rat brain after decapitation. Neurosci Lett 297: 175–118.

Thakur GA, Palmer SL, Harrington PE, Stergiades IA, Tius MA, Makriyannis A (2002). Enantiomeric resolution of a novel chiral cannabinoid receptor ligand. J Biochem Biophys Methods 54: 415–422.

Supporting information

Additional Supporting Information may be found in the online version of this article:

Figure S1 The effect of amyrins on glycerol formation in U937 cells pretreated with 10 μM JZL184. [^{3}H]-glycerol levels in U937 cells pretreated with (A) β-amyrin plus JZL184 or β-amyrin + vehicle (B) α-amyrin + JZL184 or α-amyrin + vehicle and then incubated with 1 μM 2-AG/[^{3}H]2-AG mix for 5 min. Data show means ± SEM of 12 measurements from 4 independent experiments. *P < 0.05, **P < 0.01 amyrins treated cells versus vehicle-treated cells; #P < 0.05, amyrins plus JZL184-treated cells versus amyrins plus vehicle-treated cells.